

SUPPORTING INFORMATION

Integrated Carbon Capture and Conversion to Produce Syngas: Novel Process Design, Intensification and Optimization

Shachit S. Iyer, Ishan Bajaj, Priyadarshini Balasubramanian, M. M. Faruque Hasan*

Artie McFerrin Department of Chemical Engineering, Texas A&M University
3122 TAMU, College Station, TX 77843, USA.

* Corresponding Author, Phone: (979) 862 1449; Email: hasan@tamu.edu.

S1. Non-dimensional Discretized Adsorption Model:

The process model for adsorption involves a system of partial differential equations in space and time. To solve it, the system is first discretized into a set of ordinary differential equations by applying finite volume discretization in space. Through the model is discretized using a finite volume approach, an upwind differencing scheme is used which reduces it to a finite difference approximation. Although the accuracy is reduced due to numerical dispersion, the UDS scheme is used due to its simplicity and non-oscillatory nature. The PDEs are non-dimensionalized using appropriate scaling factors for ease of convergence. The non-dimensional discretized form of the PDEs used in the adsorption model is given below:

Component mass balance:

$$\frac{\partial y_{i,j}}{\partial \tau} = \frac{1}{Pe} \frac{\bar{T}_j}{\bar{P}_j} \frac{1}{\Delta Z} \left[\left(\frac{\bar{P}}{\bar{T}} \right)_{j+0.5} \frac{(y_{i,j+1} - y_{i,j})}{\Delta Z} - \left(\frac{\bar{P}}{\bar{T}} \right)_{j-0.5} \frac{(y_{i,j} - y_{i,j-1})}{\Delta Z} \right] - \frac{\bar{T}_j}{\bar{P}_j} \frac{1}{\Delta Z} \left[\left(\frac{\bar{y}_i \bar{P}}{\bar{T}} \bar{v} \right)_{j+0.5} - \left(\frac{\bar{y}_i \bar{P}}{\bar{T}} \bar{v} \right)_{j-0.5} \right] - \psi \frac{\bar{T}_j}{\bar{P}_j} \frac{\partial \bar{q}_{i,j}}{\partial \tau} - \frac{\bar{y}_{i,j}}{\bar{P}_j} \frac{\partial \bar{P}_j}{\partial \tau} + \frac{y_i}{\bar{T}_j} \frac{\partial \bar{T}_j}{\partial \tau} \quad (S.1)$$

Total Mass balance:

$$\frac{\partial \bar{P}_j}{\partial \tau} = \frac{\bar{P}_j}{\bar{T}_j} \frac{\partial \bar{T}_j}{\partial \tau} - \frac{\bar{T}_j}{\Delta Z} \left[\left(\frac{\bar{P}}{\bar{T}} \bar{v} \right)_{j+0.5} - \left(\frac{\bar{P}}{\bar{T}} \bar{v} \right)_{j-0.5} \right] - \bar{T}_j \psi \sum_i \frac{\partial \bar{q}_i}{\partial \tau} \quad (S.2)$$

Energy Balance inside the column:

$$\begin{aligned} \frac{\partial \bar{T}_j}{\partial \tau} &= \Omega_{1,j} \frac{1}{\Delta Z} \left[\left(\frac{\bar{T}_{j+1} - \bar{T}_j}{\Delta Z} \right) - \left(\frac{\bar{T}_{j+1} - \bar{T}_j}{\Delta Z} \right) \right] - \Omega_{2,j} \frac{1}{\Delta Z} [(\bar{v} \bar{P})_{j+0.5} - (\bar{v} \bar{P})_{j-0.5}] \\ &\quad + \sum_i (\sigma_{i,j} - \Omega_{3,j} \bar{T}_j) \frac{\partial \bar{q}_i}{\partial \tau} - \Omega_{4,j} (\bar{T}_j - \bar{T}_{w,j}) - \Omega_{2,j} \frac{\partial \bar{P}_j}{\partial \tau} \end{aligned} \quad (S.3)$$

Energy Balance across the column wall:

$$\begin{aligned} \frac{\partial \bar{T}_{w,j}}{\partial \tau} &= \pi_1 \frac{1}{\Delta Z} \left[\left(\frac{\bar{T}_{w,j+1} - \bar{T}_{w,j}}{\Delta Z} \right) - \left(\frac{\bar{T}_{w,j} - \bar{T}_{w,j-1}}{\Delta Z} \right) \right] + \pi_2 (\bar{T}_j - \bar{T}_{w,j}) \\ &\quad - \pi_3 (\bar{T}_{w,j} - \bar{T}_a) \end{aligned} \quad (S.4)$$

Linear driving force model for mass transfer:

$$\frac{\partial \bar{q}_{i,j}}{\partial \tau} = \alpha_i (\bar{q}_{i,j}^* - \bar{q}_{i,j}) \quad (S.5)$$

LIST OF FIGURES

Figure S1. Temperature and CO₂ mole fraction profiles at the outlet of the adsorption column vs number of spatial discretizations

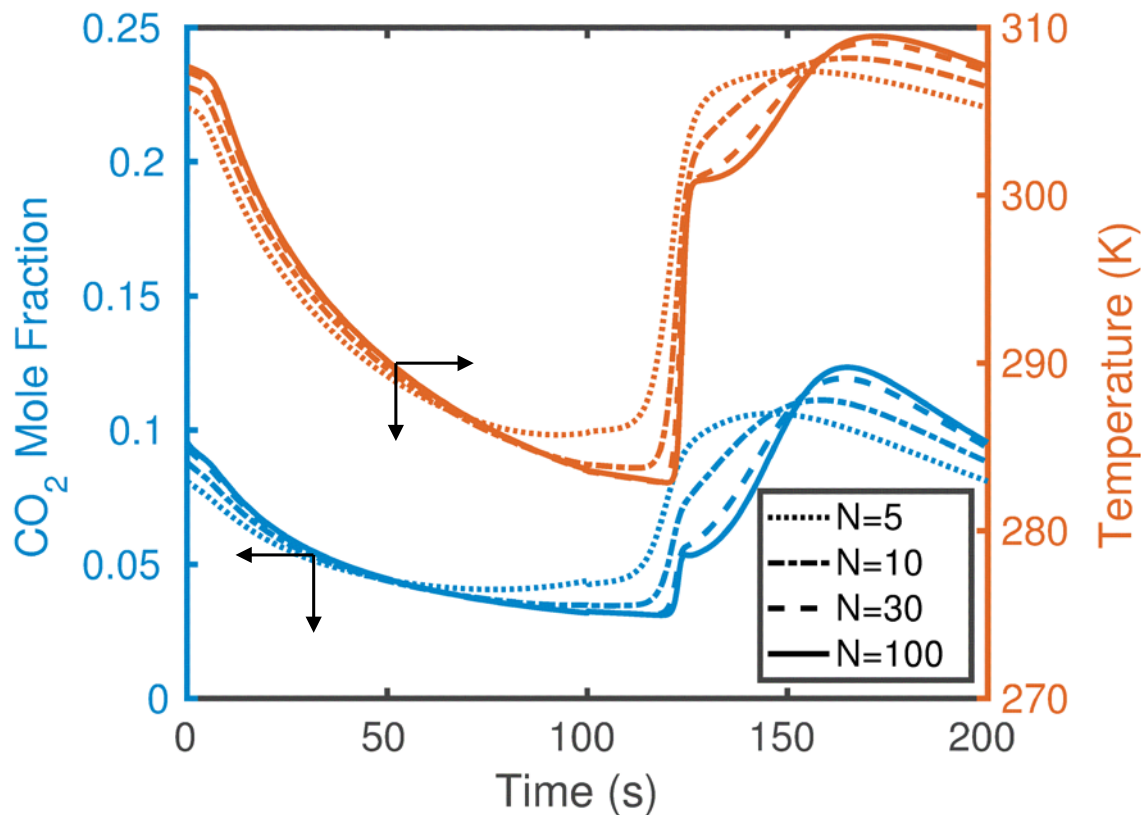


Figure S1. Temperature and CO₂ mole fraction profiles at the outlet of the adsorption column vs number of spatial discretizations. The plot shows the profiles vs the number of spatial discretizations after 100 cycles for a fixed reference case. Here N is the number of spatial discretization. The results are shown for $N= 5, 10, 30$ and 100 . With the column length fixed at 1m, these discretizations correspond to $\Delta z=0.2, 0.1, 0.033$ and 0.01 m respectively.

LIST OF TABLES

Table S1. Reaction rate coefficients and parameters.

Table S2. The individual species viscosity values in Pa s used for calculating the overall gas viscosity for the reactor section.

Table S3. Values of constants and parameters used in the model.

Table S4. Dual site Langmuir isotherm parameters fitted to experimental data from literature.

Table S5. Mole fractions in reactor outlet (product) corresponding to feed mole fractions of CO₂ and CH₄ in a binary mixture at equilibrium conditions at 1 bar and 1000 K.

Table S6. Comparison of process performance metrics obtained from short ($N=5$, $C=5$) simulations and long ($N=30$, $C=100$) simulations for the reference case.

Table S7. Algorithm parameters used in the optimization runs performed.

Table S1. Reaction rate coefficients and parameters.

Parameter	Value
k_1 [mol/kg cat/s]	$1.29 \times 10^6 e^{-102065/RT_R}$
k_2 [mol/kg cat/s]	$3.5 \times 10^5 e^{-81030/RT_R}$
$K_{CH_4,1}$ [/atm]	$2.60 \times 10^{-2} e^{40684/RT_R}$
$K_{CO_2,1}$ [/atm]	$2.61 \times 10^{-2} e^{37641/RT_R}$
$K_{CO_2,2}$ [/atm]	$0.5771 e^{9262/RT_R}$
$K_{H_2,2}$ [/atm]	$1.494 e^{6025/RT_R}$
$K_{eq,1}$ [atm ²]	$6.781 \times 10^{14} e^{-259660/RT_R}$
$K_{eq,2}$	$56.4971 e^{-36580/RT_R}$

Table S2. The individual species viscosity values in Pa s used for calculating the overall gas viscosity for the reactor section.

Species	Viscosity [Pa s]
CO	3.62 E -05
CO ₂	3.51 E -05
CH ₄	2.4 E -05
H ₂ O	3.2 E -05
H ₂	1.5 E -05
N ₂	3.5 E -05

Table S3. Values of constants and parameters used in the model.

Constants	Value
Universal gas constant R [J/mol/K]	8.314
Adsorption section model parameters	Value
Specific heat capacity of adsorbent $C_{p,s}$ [J/kg/K]	1070
Specific heat capacity of column wall $C_{p,w}$ [J/kg/K]	502
Specific heat capacity of CO ₂ [J/mol/K]	37.14
Specific heat capacity of N ₂ [J/mol/K]	29.13
Specific heat capacity of CH ₄ [J/mol/K]	35.61
Adsorbent density ρ_s [kg/m ³]	1130
Adsorption column wall density ρ_w [kg/m ³]	7800
Inside heat transfer coefficient h_{in} [J/m ² /K/s]	8.6
Outside heat transfer coefficient h_{in} [J/m ² /K/s]	2.5
Viscosity of gas in adsorption column μ [kg/m/s]	1.72 E -05
Molecular diffusivity D_m [m ² /s]	1.6 E -05
Thermal conductivity of column wall K_w [J/m/K/s]	16
Effective gas thermal conductivity K_z [J/m/K/s]	0.09
Adsorbent column void fraction ε	0.37
Adsorbent particle porosity ε_p	0.54
Adsorbent particle radius r_p [m]	1.6 E -03
Adsorbent tortuosity τ'	3
Reactor section model parameters	Value
Reactor bed density ρ_b [kg/m ³]	900
Catalyst particle diameter d_p [m]	0.019
Catalyst particle length d_l [m]	0.016
Number of hole rings in the catalyst particle n_h	10
Diameter of the hole rings r_h [m]	0.0023
Void fraction of reactor bed ε_R	0.4

Table S4. Dual site Langmuir isotherm parameters fitted to experimental data from literature.

Parameter	Value	Parameter	Value	Parameter	Value
$b_{CO_2}^0$ [m ³ /mol]	1 E -09	$b_{N_2}^0$ [m ³ /mol]	4.32 E -06	$b_{CH_4}^0$ [m ³ /mol]	6.29 E -06
$d_{CO_2}^0$ [m ³ /mol]	2.63 E -07	$d_{N_2}^0$ [m ³ /mol]	2.65 E -06	$d_{CH_4}^0$ [m ³ /mol]	1.84 E -06
q_{b,CO_2}^s [mol/m ³]	4997.764	q_{b,N_2}^s [mol/m ³]	10557.477	q_{b,CH_4}^s [mol/m ³]	4616.276
q_{d,CO_2}^s [mol/m ³]	5800.516	q_{d,N_2}^s [mol/m ³]	3674.76	q_{d,CH_4}^s [mol/m ³]	16950.00
$\Delta U_{b,CO_2}$ [J/mol]	-33917.46	$\Delta U_{b,N_2}$ [J/mol]	-8089.09	$\Delta U_{b,CH_4}$ [J/mol]	-15922.30
$\Delta U_{d,CO_2}$ [J/mol]	-31731.06	$\Delta U_{d,N_2}$ [J/mol]	-16361.22	$\Delta U_{d,CH_4}$ [J/mol]	-9465.77

Table S5. Mole fractions in reactor outlet (product) corresponding to feed mole fractions of CO₂ and CH₄ in a binary mixture at equilibrium conditions at 1 bar and 1000 K. This result is obtained based on Gibbs energy minimization performed using Aspen Plus RGIBBS module to demonstrate that the feed composition significantly affects the product composition.

CO ₂ in Feed	CH ₄ in Feed	CO ₂ in Product	CH ₄ in Product
0.095	0.86	5.52 E-05	0.64
0.27	0.69	0.003	0.28
0.39	0.57	0.013	0.13
0.48	0.49	0.032	0.06
0.54	0.43	0.06	0.03

Table S6. Comparison of process performance metrics obtained from short ($N=5$, $C=5$) simulations and long ($N = 30$, $C = 100$) simulations for the reference case. The absolute value of the percentage deviation of the short simulations from the longer simulations is also reported.

Process Metric	$N = 30, C = 100$	$N=5, C=5$	% Deviation
% CO ₂ Utilization	75.63	76.44	1.07
Total Cost (\$/ton SG)	218.06	221.27	1.47
Operating Cost (\$/ton SG)	175.33	178.03	1.54
Total loss % CH ₄	62.62	62.86	0.38
Total loss % CO ₂	24.29	23.49	3.29
Vent loss % CH ₄	4.26	5.05	18.54
Vent loss % CO ₂	3.14	3.00	4.46
Unreacted % CH ₄	58.36	57.82	0.93
Unreacted % CO ₂	21.16	20.49	3.17
Syngas ratio (H ₂ /CO)	0.83	0.83	0
CH ₄ % in product	0.25	0.25	0
CO ₂ % in product	0.05	0.05	0
N ₂ % in product	0.03	0.03	0
H ₂ % in product	0.29	0.29	0
CO % in product	0.35	0.35	0
H ₂ O % in product	0.03	0.03	0

Table S7. Algorithm parameters used in the optimization runs performed. L₁ norm is used for defining trust region size.

Algorithm Parameters	Values
Constraint violation tolerance (θ^{tol})	0
Root mean squared error tolerance (ε^{tol})	10^{-3}
Threshold value for criticality measure (φ^{tol})	10^{-3}
Minimum trust region size (Δ^{min})	10^{-5}
Trust region decrease factor (γ_{dec})	0.5
Trust region increase factor (γ_{inc})	3
Ratio of actual decrease and predicted decrease in objective function (η)	0.25